

Slugging in multiphase flow as a mixed initial-boundary value problem for a quasilinear hyperbolic system

Florent Di Meglio, Glenn-Ole Kaasa, Nicolas Petit, Vidar Alstad

Abstract—This paper studies the multiphase slugging flow phenomenon occurring in oil wells and flow lines. The main contribution is a low-dimensional distributed parameters model, comprising the gas mass fraction, the pressure, and gas velocity as states. Along with appropriate boundary conditions, on the one-dimensional space domain, it constitutes a well-posed mixed initial-boundary value problem for a quasilinear hyperbolic system. Numerical simulation results obtained with a presented characteristics method solver stress the validity of the approach and the fair representativeness of the model. In particular, the period of simulated oscillations and their overall shape is in accordance with reference results from the literature. Controllability and observability open problems are formulated for future works.

I. INTRODUCTION

In this article, we propose a model of the slugging phenomenon taking the form of a low-dimensional hyperbolic system of conservation laws. Slugging is a two-phase flow regime occurring during the process of oil production. In certain circumstances, the inhomogeneous repartition of gas and liquid into the long transport pipes leads to this oscillating flow pattern, which is detrimental to the overall production and is at the source of severe issues concerning safety of operations. The physical description of this phenomenon is as follows. Elongated bubbles of gas, separated by “slugs” travel from one end of a pipe to the other. This results in large pressure oscillations and an intermittent flow. A main negative effect is that the average (over time) production of oil is decreased compared to steady flow regimes.

Modeling this phenomenon is a difficult task, because its origins are not completely understood yet. Early models have focused on the transitions between flow patterns [31] or the prediction of the flow characteristics (e.g. average liquid hold-up, pressure drop...) [1]. More recently, distributed parameters models have been developed in commercial simulation softwares, such as OLGATM or TACITETM. They are based on nonlinear Partial Differential Equations (PDEs), and reproduce with a good accuracy the dynamical behavior of slugging wells. However, even if they rely on well-documented physics and modeling assumptions, their “black-box” nature (for the end-user) and the high dimensionality

of the state equations make these softwares hardly usable for mathematical analysis, let alone control design.

Conversely, reduced models have been developed [8], [24], [30]. They are based on nonlinear Ordinary Differential Equations (ODEs) and capture the main features of the slugging oscillations. Their relative simplicity makes them suitable for control (and observer) design, at the expense of sometimes tedious tuning procedures aimed at reproducing field data (see, e.g., [10]). These models rely on restrictive modeling assumptions which, in turn, might seem inappropriate from a physical modeling view-point. The Jansen model [24] is designed specifically for gas-lifted wells, whereas the Storkaas model [30] corresponds to risers with a low-point. The model proposed in [8] assumes the existence of an irregularity in the pipe geometry at the birth of instability.

In this article, we propose a low-dimensional model which is minimal, in the sense that no assumptions are made on the geometry or setup of the system, and that it reproduces with a fair accuracy observed behaviors. Following many other modeling works (e.g. [1], [3], [12], [16]), the drift-flux approach is used. This implies that the momentum equations for the gas and the liquid are combined into a single one, and that an affine slip relation with constant parameters relates the velocities of the two phases. Importantly, this is the only empirical relation used in the model. The approach is very similar to the density wave model of Sinègre [28], which was first described and illustrated by OLGA simulations in [22]. In [28], a distributed parameters model was provided, along with a thorough stability analysis, describing the phenomenon. Yet, the analysis relies on simplifications which preserve the stability properties, but may hurt the physical interpretation¹.

The main contribution of this article is a low-dimensional model of slugging phenomenon taking the form of a hyperbolic system of conservation laws, with a one-sided boundary actuation. The advantages of such a formulation are two-fold. First, it is consistent with recent mathematical tools of analysis of PDE control systems, e.g. results that guarantee well-posedness of the problem. Similarly, theoretical controllability and observability results might be used. Such problems of well-posedness and boundary control of hyperbolic systems have been widely studied [6], [25], [26]. Second, the method of characteristics (see [2], [5], [27] for application to hyperbolic control systems) can be used to numerically solve the equations, which reduces the compu-

F. Di Meglio (corresponding author) is a PhD candidate in Mathematics and Control at MINES ParisTech, 60, Bd St-Michel, 75272 Paris, Cedex 06, France

G.O. Kaasa is Research Engineer at StatoilHydro ASA, Research Center Porsgrunn, Heroya Forskningspark 3908 Porsgrunn, Norway

N. Petit is Professor at MINES ParisTech, 60, Bd St-Michel, 75272 Paris, Cedex 06, France

V. Alstad is Research Engineer at Statoil ASA, Research Center Porsgrunn, Heroya Forskningspark 3908 Porsgrunn, Norway

¹In particular, the gas velocity is assumed constant in time and space, which is not realistic in practice. No such assumption is made here.

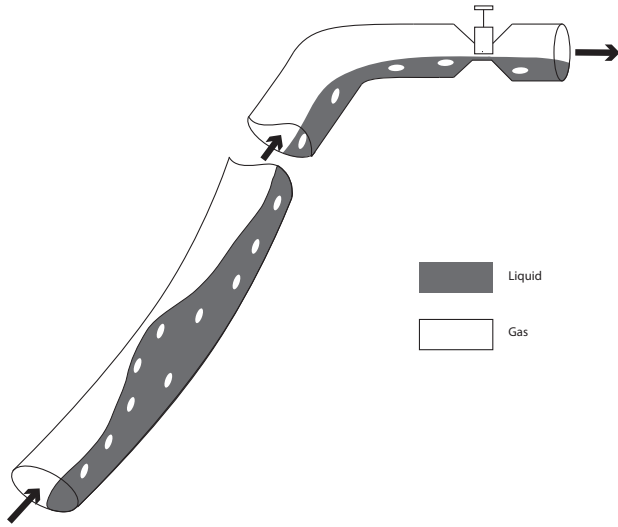


Fig. 1. Inclined pipe transporting oil and gas

tational burden. As illustrated by simulations, the proposed model has the ability to reproduce oscillations corresponding to the slugging phenomenon.

The paper is organized as follows. In Section II, we introduce the distributed parameters model and the boundary conditions, from a physical view-point. Then, in Section III, we proceed to a state transformation and show well-posedness of the mixed-initial boundary value problem. Controllability and observability problems are discussed. Further, a numerical solver is presented in Section IV, along with simulations which illustrate the relevance of our approach. Conclusions are given in Section V.

II. MODELING - THE PHYSICS

We consider the multiphase flow of gas and oil through an inclined circular cross-section pipe as depicted in Figure 1. The gas and liquid flow from the reservoir into the pipe, and eventually reach a remotely controlled valve (“production choke”) before being separated in the downstream facilities.

A. Conservation laws

Following the classical drift-flux approach ([4], [12], [15]), the model equations consist of two mass conservation laws, for the gas and the liquid, respectively, and a combined momentum equation. The flow is assumed to be one-dimensional. Thus, the radial and angular variations of all physical quantities are neglected. This yields the following system of PDEs

$$\frac{\partial \alpha_G \rho_G}{\partial t} + \frac{\partial \alpha_G \rho_G v_G}{\partial z} = 0 \quad (1)$$

$$\frac{\partial \alpha_L \rho_L}{\partial t} + \frac{\partial \alpha_L \rho_L v_L}{\partial z} = 0 \quad (2)$$

$$\frac{\partial \alpha_G \rho_G v_G + \alpha_L \rho_L v_L}{\partial t} + \frac{\partial P + \alpha_G \rho_G v_G^2 + \alpha_L \rho_L v_L^2}{\partial z} = F_G^W + F_L^W - \rho_m g \sin \theta(z) \quad (3)$$

where, for $k = G$ or L , α_k denotes the volume fraction of phase k , ρ_k denotes its density, and v_k its velocity. P denotes the pressure, ρ_m is the density of the mixture and F_k^W accounts for the friction of phase k against the pipe walls. The two following physical definitions hold

$$\alpha_G + \alpha_L = 1 \quad \text{and} \quad \rho_m = \alpha_G \rho_G + \alpha_L \rho_L \quad (4)$$

In (3), $\theta(z)$ is the inclination of the pipe. The time variable is $t > 0$ and $z \in [0, L]$ is the space variable, where L is the total length of the pipe. In order to put the system in a conservative form, several additional relations are needed. Then, two empirical relations, given below, allow to “close” the system.

a) *Ideal gas*: The gas is supposed to satisfy the ideal gas law, which (locally) reads $P = \rho_G R T$, where R is the specific gas constant, and T is the temperature. The pressure at one location in the pipe is assumed to be equal to the pressure in the gas phase.

b) *Slip relation*: Following [28], the velocities of gas and liquid are assumed to satisfy the following slip relation

$$v_G - v_L = \frac{v_\infty}{\alpha_L} \quad (5)$$

where v_∞ is a *constant* parameter. In most drift-flux models (e.g. [12], [19]), the parameter v_∞ depends on the state of the system, according to empirical laws depending on the flow regime under consideration (annular, dispersed, stratified, respectively). Yet, in [28], it was shown that the slugging oscillations could be fairly reproduced in a multiphase simulator, even with a constant v_∞ . We follow this approach.

Eventually, the following simplifying assumptions are made

c) *Incompressible oil*: The oil is assumed to be incompressible, which implies that $\rho_L(t, z) = \rho_L = \text{cst}$. This is a classical assumption, as the oil is a liquid phase.

d) *Neglectible friction*: The friction against the walls is assumed to be neglectible compared to gravity ($F_G^W = F_L^W = 0$). This is a reasonable assumption as severe slugging is known to be a gravity-dominated phenomenon [30].

B. Boundary conditions

The boundary conditions are given at both ends of the pipe. At the bottom, the flow of liquid is assumed to linearly depend on the pressure drop between the pipe and the oil reservoir (alternatively, other sources of oil could be considered as well). Then,

$$\begin{aligned} \Phi_L(t, z = 0) &= \alpha_L(t, z = 0) \rho_L v_L(t, z = 0) \\ &= \text{PI} [P_r - P(t, z = 0)] \end{aligned} \quad (6)$$

In (6), the constant coefficient PI is called the Productivity Index. The pressure in the reservoir P_r is assumed to be constant. Also, at the bottom end of the pipe, the flow of gas is assumed to be constant too

$$\Phi_G(t, 0) = \alpha_G(t, 0) \rho_G(t, 0) v_G(t, 0) = \Phi_G \quad (7)$$

Eventually, at the top, the total outflow is assumed to be governed by a multiphasic valve equation of the (general) form

$$\begin{aligned}\Phi_L(L) + \Phi_G(L) &= \alpha_L(L) \rho_L v_L(L) + \alpha_G(L) \rho_G(L) v_G(L) \\ &= C_{pc} Z \sqrt{\rho_m(L) (P(L) - P_s)}\end{aligned}\quad (8)$$

where P_s is the constant pressure in the separator. The valve (or ‘‘choke’’) opening Z is the control input. The choke is remotely actuated. Its opening can be continuously adjusted to control the flow, e.g. to stabilize it using feedback loops. Note that, in (8), the time variable is omitted for readability.

III. A WELL-POSED MIXED INITIAL-BOUNDARY VALUE PROBLEM

As is, the system (1)-(2)-(3) is in implicit form, which is hardly suitable for any mathematical analysis. In order to prove well-posedness of the problem, we re-formulate the conservation equations as a hyperbolic system of PDE. After a suitable transformation of the boundary conditions, this allows to consider the well-posedness of a mixed initial-boundary value problem, applying results from [26]. Further, even though no results on boundary controllability or observability are applicable as for now, the results obtained in finite dimension [9], [13], suggest that boundary stabilizability or observability could be obtained. We propose two such problems for future works.

A. Well-posedness

a) *Hyperbolic system:* Consider the following state vector

$$u = \begin{pmatrix} u_1 & u_2 & u_3 \end{pmatrix}^T = \begin{pmatrix} \frac{\alpha_G \rho_G}{\alpha_G \rho_G + \alpha_L \rho_L} & \frac{P}{\text{bar}} & v_G \end{pmatrix}^T$$

where the pressure is divided by $1 \text{ bar} = 1 \times 10^5 \text{ Pa}$ to ensure, later, proper numerical conditioning of the solver². Combining equations (1)-(2)-(3), and the static relations (4) and (5) allows to rewrite the system in conservative form

$$\frac{\partial H(u)}{\partial t} + \frac{\partial F(u)}{\partial z} = G(z, u) \quad (9)$$

Then, noticing that $\frac{\partial H(u)}{\partial t} = H'(u) \frac{\partial u}{\partial t}$, one obtains

$$\frac{\partial u}{\partial t} + A(u) \frac{\partial u}{\partial z} = S(z) \quad (10)$$

where $A(u) = H'(u)^{-1} F'(u)$ and³ $S(z) = H'(u)^{-1} G(z, u)$. The expressions of $A(u)$ and S are given in Appendix. To guarantee that A and all the other functions of u belong to C^1 , we restrict our study to a compact set

$$u \in K \subset (0, 1) \times (P_s, P_r) \times (0, +\infty) \subset \mathbb{R}^3$$

For each value of $u \in K$, A has 3 real eigenvalues $\lambda_i(u)$, $i = 1, 2, 3$, as well as a set of linearly independent left eigenvectors $l(u) = \begin{pmatrix} l_1(u) \\ l_2(u) \\ l_3(u) \end{pmatrix}$ (such that $\forall u, i, l_i(u) A(u) = \lambda_i(u) l_i(u)$). This implies that system (10) is hyperbolic, e.g.

²this is certainly unnecessary for the theoretical study

³A cancellation of the state-dependent terms occurs in the derivation of S which allows to write $S(z)$ instead of $S(z, u)$.

according to the definition given in [26, p. 195]. One should notice that u_1 is a Riemann invariant for the system, as it is the case in the model of [28]. Moreover, all the numerical applications that we have performed so far have shown that the following inequalities hold

$$\forall u, \quad \lambda_1(u) < 0 < \lambda_2(u) < \lambda_3(u) \quad (11)$$

some of which are difficult to prove by mathematical analysis given the complexity of the expressions of the λ_i . This ensures that the system is strictly hyperbolic.

b) *Boundary conditions:* In order to establish the well-posedness of the mixed initial-boundary value problem, the boundary conditions (6)-(7)-(8) must be rewritten. More precisely, given a C^1 initial condition

$$\varphi : [0, L] \rightarrow K \quad (12)$$

there must exist two functions $g_l : \mathbb{R} \rightarrow \mathbb{R}^2$ and $g_r : \mathbb{R}^2 \rightarrow \mathbb{R}$ such that Equations (6)-(7)-(8) are equivalent⁴ to

$$\begin{cases} z = 0 : & \begin{pmatrix} \tilde{v}_2(t, 0) & \tilde{v}_3(t, 0) \end{pmatrix}^T = g_l(\tilde{v}_1(t, 0)) \\ z = L : & \tilde{v}_1(t, L) = g_r(\tilde{v}_3(t, L), \tilde{v}_2(t, L), Z) \end{cases} \quad (13)$$

where

$$\tilde{v}(t, z) = l(\varphi(z))u(t, z)$$

and Z is the control input. The existence of such functions only depends on the choice of the initial condition φ . This is due to the fact that the number of equations at each boundary is consistent with the sign of the eigenvalues (11). Indeed, there are two equations at the boundary $z = 0$, which correspond to the two positive eigenvalues, and one equation at $z = L$ corresponding to $\lambda_1 < 0$. Yet, this does not guarantee that the boundary conditions can be inverted with respect to the components of \tilde{v} (i.e., that the Implicit Functions Theorem applies). We now give necessary and sufficient conditions for the existence of g_l and g_r . First, let us rewrite Equations (6)-(7)-(8) in the u variables. We omit the time and space arguments for readability. The left boundary conditions ($z = 0$) read

$$\begin{aligned} h_l(u_1, u_2, u_3) &= \begin{pmatrix} \rho_L u_1 u_2 u_3 \text{bar} - \Phi_G [\rho_L R T u_1 + (1 - u_1) u_2 \text{bar}] \\ \Phi_G - u_1 [\Phi_g + \rho_L v_\infty + P I(p_r - u_2)] \end{pmatrix} \\ &= 0 \end{aligned} \quad (14)$$

while the right boundary condition reads

$$\begin{aligned} h_r(u_1, u_2, u_3, Z) &= \frac{\rho_L u_2 u_3 \text{bar}}{\rho_L R T u_1 + (1 - u_1) u_2 \text{bar}} - v_\infty \rho_L \\ &\quad - C_c Z \sqrt{\frac{\rho_L u_2 u_3 \text{bar}}{\rho_L R T u_1 + (1 - u_1) u_2 \text{bar}}} (u_2 - p_s) \\ &= 0 \end{aligned} \quad (15)$$

In the \tilde{v} variables, these can be rewritten

$$z = 0 : \quad \tilde{h}_l(\tilde{v}_1, \tilde{v}_2, \tilde{v}_3) = h_l(m_1 \tilde{v}, m_2 \tilde{v}, m_3 \tilde{v}) = 0$$

⁴following the standard notations of [26]

and

$$z = L : \quad \tilde{h}_r(\tilde{v}_1, \tilde{v}_2, \tilde{v}_3, Z) = h_r(m_1\tilde{v}, m_2\tilde{v}, m_3\tilde{v}, Z) = 0$$

where the m_i are line vectors such that $(m_i)_{i=1,2,3} = l^{-1}$. A necessary and sufficient condition for the functions g_l and g_r to exist is that the following partial Jacobian matrices

$$\left(\begin{array}{ccc} \frac{\partial \tilde{h}_l}{\partial \tilde{v}_2}(\tilde{v}_1(0), \tilde{v}_2(0), \tilde{v}_3(0)) & \frac{\partial \tilde{h}_l}{\partial \tilde{v}_3}(\tilde{v}_1(0), \tilde{v}_2(0), \tilde{v}_3(0)) \end{array} \right)$$

and

$$\left(\begin{array}{ccc} \frac{\partial \tilde{h}_r}{\partial \tilde{v}_1}(\tilde{v}_1(L), \tilde{v}_2(L), \tilde{v}_3(L)) \end{array} \right)$$

are nonsingular. This yields the following necessary and sufficient conditions for the existence of g_l and g_r : the initial condition φ must be such that, for any $u(z) = (u_1(z) \ u_2(z) \ u_3(z))^T$ verifying Equations (14) and (15)

$$\det \left| \frac{\partial h_l}{\partial u}(u(0)) \begin{pmatrix} m_{12}(\varphi(0)) & m_{13}(\varphi(0)) \\ m_{22}(\varphi(0)) & m_{23}(\varphi(0)) \\ m_{32}(\varphi(0)) & m_{33}(\varphi(0)) \end{pmatrix} \right| \neq 0$$

and

$$\frac{\partial h_r}{\partial u}(u(L)) \begin{pmatrix} m_{11}(\varphi(L)) \\ m_{21}(\varphi(L)) \\ m_{31}(\varphi(L)) \end{pmatrix} \neq 0 \quad (16)$$

If $\varphi(z)$ verifies these conditions, then the Implicit Function Theorem guarantees the existence of g_l and g_r . Further, the well-posedness follows, according to Theorem A.2 in [26], given that $\varphi(z)$ also verifies conditions of C^1 compatibility.

More precisely, this theorem guarantees that there exists $\delta > 0$ such that the hyperbolic system (10) with initial condition (12) and boundary conditions (13) admits a unique local C^1 solution $u = u(t, z)$ on the domain

$$\{(t, z) \mid 0 \leq t \leq \delta, \ 0 \leq z \leq L\}$$

B. Remarks on stabilizability and observability

As recalled in [11], the stabilization of the slugging phenomenon has been studied since as early as 1930. Of the many solutions proposed to suppress the oscillations, automatic control of the production choke is the one that has prevailed. Many successful implementations of various controllers have been reported since [21], [7], [20], [17]. These controllers all use pressure sensors in feedback loop to stabilize the flow by production choke actuation. Yet, theoretical analysis of the controllability of slugging systems has only appeared much later, with Imsland [23], Storkaas [30] and Sinègre [28]. Their results only hold for finite-dimensional models, and no result exists, to our knowledge, on the controllability of a PDE model for slugging.

Similarly, the difficulty of placing sensors at deep locations has motivated investigations on observers using only topside (and thus, easily accessible) measurements to estimate the pressure everywhere in the pipe. Eikrem [14] and Sinègre [28] provide examples of successfully implemented observers, where the masses of gas and liquid inside the pipes are dynamically estimated. Again, these results rely on ODE models.

The industrial problem of controlling (resp. estimating) the flow thanks to production choke actuation (resp. topside measurements) translates, in the framework of this article, into the one-sided boundary control (resp. observation) of the strictly-hyperbolic system (10). The actuator is located at boundary $z = L$, and the control law must be defined by partially inverting function g_r in Equation (15) with respect to Z .

The most advanced results on these topics are found in [25] and [26], where both the problems of one-sided boundary controllability and observability of quasilinear hyperbolic systems are addressed. However, Li's [26] results all impose requirements on the signs of the eigenvalues. More precisely, to have controllability (resp. observability) by acting on the boundary condition at $z = L$, the number of positive eigenvalues must be less than the number of negative eigenvalues. These conditions are not fulfilled in the case of slugging, as there are two positive eigenvalues, and one negative (see (11)). However, these conditions are only necessary, and milder results could be investigated with our setup. Indeed, Li's results concern the *exact* controllability and observability of the whole state of the PDE. For industrial purposes, this is neither needed nor realistic. Stabilizability and detectability would probably be more suitable objectives.

Recently, works by Krstic [25] have focused on the boundary null control of a single hyperbolic PDE, with constant (possibly unknown) propagation speed. These results do not directly apply here either, as the phenomenon is genuinely nonlinear (and state-dependent speed) in its propagation, and consists of a coupled set of equations. However, the backstepping approach could be used to obtain stabilizability results for the considered problem.

To summarize the above discussion, the two following problems could be considered and are of practical interest

Problem 3.1: Consider Equation (10) with boundary conditions (13), where Z is the control input. Given $\bar{u}(z)$ an equilibrium profile, and φ an initial condition close to \bar{u} , is there a feedback law $Z = \psi(u_1, u_2, u_3)$ such that \bar{u} is a stable equilibrium?

Concerning observability, we formulate a similar problem

Problem 3.2: Consider Equation (10) with boundary conditions (13), with a constant known input Z . Assuming that the topside pressure $u_2(t, z = L)$ is measured, can one construct an observer \hat{u} such that $\hat{u}_2(t, z = 0) \xrightarrow{t \rightarrow +\infty} u_2(t, z = 0)$?

IV. NUMERICAL VALIDATION

In this section, we illustrate the relevance of the proposed model by numerical simulations. The main result is that the model is able to reproduce the oscillations corresponding to the slugging behavior. The solution of the mixed initial-boundary value problem is computed using the method of characteristics.

A. Method of characteristics

The method is based on the following transformation of the equations. Let u be a C^1 solution of system (10) with

boundary conditions (13). For $i = 1, 2, 3$, let $\zeta_i : t > 0 \mapsto \zeta_i(t) \in [0, L]$ be such that

$$\frac{d\zeta_i}{dt}(t) = \lambda_i(u(t, \zeta_i(t))) \quad (17)$$

The existence of such functions is guaranteed by the Cauchy-Lipschitz theorem (see e.g. [18]). Now, consider the functions $\gamma_i : t \mapsto u(t, \zeta_i(t))$. For each i , γ_i verifies the scalar equation

$$\begin{aligned} l_i(\gamma_i) \frac{d\gamma_i}{dt} &= l_i(\gamma_i) \left(\frac{\partial u}{\partial t}(t, \zeta_i(t)) + \frac{d\zeta_i}{dt} \frac{\partial u}{\partial z}(t, \zeta_i(t)) \right) \\ &= l_i(\gamma_i) \left(\frac{\partial u}{\partial t}(t, \zeta_i(t)) + \lambda_i(\gamma_i) \frac{\partial u}{\partial z}(t, \zeta_i(t)) \right) \\ &= l_i(\gamma_i) \left(\frac{\partial u}{\partial t}(t, \zeta_i(t)) + A(\gamma_i) \frac{\partial u}{\partial z}(t, \zeta_i(t)) \right) \\ &= l_i(\gamma_i) \left(\frac{\partial u}{\partial t}(t, \zeta_i(t)) + A(u(t, \zeta_i(t))) \frac{\partial u}{\partial z}(t, \zeta_i(t)) \right) \\ &= l_i(\gamma_i) S(\zeta_i) \end{aligned}$$

This yields the following propagation equations, for $i = 1, 2, 3$

$$l_i(u(t, \zeta_i(t))) \left(\frac{du(t, \zeta_i(t))}{dt} - S \right) = 0 \quad (18)$$

The curves $(t, \zeta_i(t))$ in the \mathbb{R}^2 plane are called characteristic curves, and Equations (17) are referred to as the characteristic equations. Along these curves, the system is reduced to a set of 3 coupled Ordinary Differential Equations. This induces the following numerical scheme.

B. Numerical scheme

Consider the discretized time-space grid $\{t \in \{0, \Delta t, \dots, n\Delta t, \dots\}, z \in \{0, \Delta z, \dots, k\Delta z, \dots, L\}\}$. The time and space steps Δt and Δz are constant, and we assume that the Courant-Friedrichs-Lewy condition

$$\max_{i=1,2,3} \lambda_i(u) < \frac{\Delta z}{\Delta t} \quad (19)$$

is always verified, namely, for all values of the solution u (therefore in each block). The Euler-scheme discretized equations corresponding to the characteristic equations (17) and the propagation equations (18) read

$$\frac{\zeta_i(n+1) - \zeta_i(n)}{\Delta t} = \lambda_i(u(n, \zeta_i(n))) \quad (20)$$

and

$$l_i(u(n, \zeta_i(n))) \left(\frac{u(n+1, \zeta_i(n+1)) - u(n, \zeta_i(n))}{\Delta t} - S \right) = 0 \quad (21)$$

Let us assume that the solution is known at time $t = t_0 + n\Delta t$ for all $z \in \{0, \Delta z, \dots, k\Delta z, \dots, L\}$. We now detail how to determine the solution at time $t + \Delta t$, and location $z = k\Delta z$.

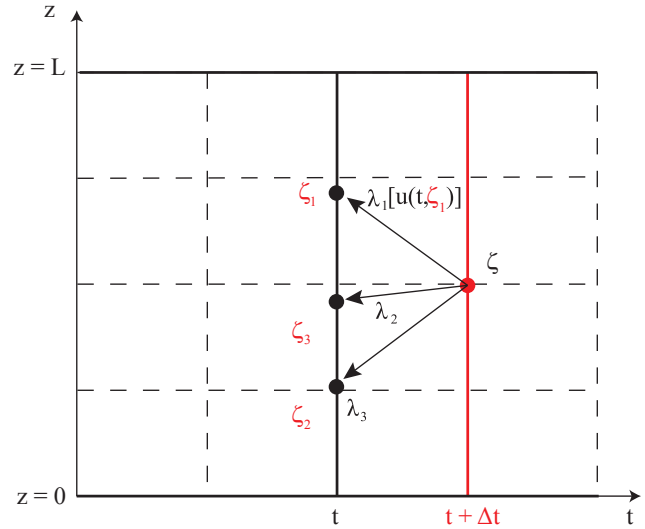


Fig. 2. Solving of the discrete characteristic equations backward in time.

c) *Case 1: $k \neq 0, \frac{L}{\Delta z}$* : We consider the characteristic curves passing through the point $(t + \Delta t, z)$. According to (20), their discretized equations read $\frac{z - \zeta_i(n)}{\Delta t} = \lambda_i(u(n, \zeta_i(n)))$, where the $\zeta_i, i = 1, 2, 3$ are unknowns to be determined. This is done by applying Newton's algorithm to find the solution to the 3 equations

$$\psi(\zeta_i) = z - \zeta_i - \Delta t \lambda(u(n, \zeta_i)) = 0 \quad (22)$$

This point is illustrated on Figure 2. One should notice that the CFL conditions (19) guarantee that $\forall i \ z - \Delta z < \zeta_i < z + \Delta z$. Also, the solution is known at time t for all $z = k\Delta z$, but the algorithm uses the values of the λ_i and $\frac{d\lambda_i}{dz}$ at locations which are not exactly on the grid. The interpolation methods used to compute these intermediate values are discussed in details in Section IV-C.

Once the $\zeta_i, i = 1, 2, 3$ have been determined, they can be used to find the value of the solution at the point $(t + \Delta t, z)$. Indeed, Equations (21) can be rewritten as

$$u(n+1, z) = \begin{pmatrix} l_1(u(n, \zeta_1)) \\ l_2(u(n, \zeta_2)) \\ l_3(u(n, \zeta_3)) \end{pmatrix}^{-1} \begin{pmatrix} l_1(u(n, \zeta_1)) [u(n, \zeta_1) + \Delta t S] \\ l_2(u(n, \zeta_2)) [u(n, \zeta_2) + \Delta t S] \\ l_3(u(n, \zeta_3)) [u(n, \zeta_3) + \Delta t S] \end{pmatrix} \quad (23)$$

This explicit formula requires the values of the solution at locations $\zeta_i, i = 1, 2, 3$. Again, these points are unlikely to be exactly at grid points, and interpolation is needed (see Section IV-C).

d) *Case 2: $k=0$* : In this case, the two characteristic curves corresponding to positive eigenvalues leave the domain. The corresponding propagation equations are replaced by the boundary conditions (6) and (7). After having solved the characteristic equation corresponding to $\lambda_1 < 0$ and having computed ζ_1 , this yields the following system to be

solved

$$\psi_I(u_1, u_2, u_3) = \begin{pmatrix} l_1(u(n, \zeta_1)) \begin{bmatrix} u_1 \\ u_2 \\ u_3 \end{bmatrix}^T - u(n, \zeta_1) - \Delta t S \\ \rho_L u_1 u_2 u_3 \text{bar} - \Phi_G [\rho_L R T u_1 + (1 - u_1) u_2 \text{bar}] \\ \Phi_G - u_1 [\Phi_g + \rho_L v_\infty + P I(p_r - u_2)] \end{pmatrix} = \begin{pmatrix} 0 \\ 0 \\ 0 \end{pmatrix} \quad (24)$$

This system of nonlinear equations is solved, again, using Newton's algorithm.

e) *Case 3*: $k = \frac{L}{\Delta z}$: Similarly, in this case, the characteristic curve corresponding to $\lambda_1 < 0$ exits the domain. It is replaced by the right boundary condition. Again, this yields a system of 3 equations which is solved using Newton's algorithm.

The aforescribed method allows to compute the values at time $t + \Delta t$, for all locations $k\Delta z$, provided that the solution is known at time t . In this numerical scheme, the estimation of the value of the solution between the nodes of the grid is of great importance. This is the topic of the next paragraph.

C. Interpolation methods

The interpolation method used to compute the value of the solution and the eigenvalues between the nodes of the grid is crucial to obtain the convergence of the numerical scheme. A malicious effect implied by the usage of insufficiently accurate interpolation is the generation of spurious oscillations, especially close to the boundaries of the spatial domain where steep gradients can be observed. This point was investigated by Tsai [32], who uses cubic Hermite splines with estimates of the spatial derivative of the solution. These are provided by additional PDEs to solve. His method provides a good accuracy at the expense of and increased computational complexity. In this article, the intermediate values are computed using the following three points Lagrange interpolation formula

$$f(z_0 + p\Delta z) = \frac{p(p-1)}{2} f(z_0 - \Delta z) + (1-p^2) f(z_0) + \frac{p(p+1)}{2} f(z_0 + \Delta z)$$

with $|p| \leq 1$. In particular, when computing the value of the solution at point $(t + \Delta t, z)$, one has to evaluate the solution at point (t, ζ_i) , with $z - \Delta z < \zeta_i < z + \Delta z$. The formula is used by setting $p = \frac{\zeta_i - z}{\Delta z}$.

D. Simulations

The model was tested on a 2500-meter long vertical well. The simulation was initialized at the equilibrium, with a fully opened production choke $Z = 100\%$. The time step was chosen to be $\Delta t = 0.01$ s and the space step was set to $\Delta z = 61.25$ m. A typical value of the largest eigenvalue is $|\lambda_1| \approx 300 \text{ m}\cdot\text{s}^{-1}$, so that the CFL conditions are satisfied. After a time $t = 5$ h, the production choke was gradually closed to $Z = 60\%$. Then, after 7 more hours, the production choke was closed to $Z = 20\%$. The resulting variations of

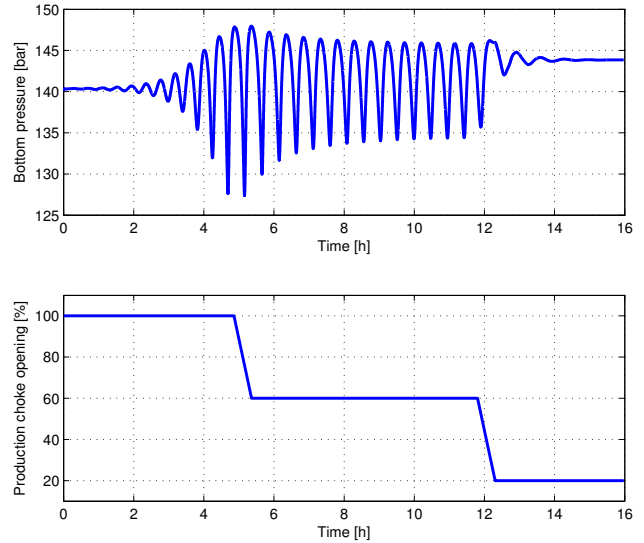


Fig. 3. Variations of the bottom side pressure and production choke opening. At $Z = 20\%$, the system is stable.

the bottom side pressure are pictured in Figure 3. The period of the oscillations is approximately 30 minutes, which is in accordance with the results of [29], for a similar well. Moreover, the model reproduces an important feature of slugging wells. It is a well-known fact that choking down the well, i.e. reducing the opening of the production valve, stabilizes the flow (at the expense of the production level, which then decreases). This behavior was proved to correspond to a Hopf bifurcation in [33], the system switching stability as the choke opening decreases. As pictured on Figure 3, the bifurcation point for this system is located between a 20% and 60% choke opening. To illustrate the mechanism of the oscillations, "snapshots" of the liquid mass hold-up profiles over one slugging cycle are pictured on Figure 4. Also note that the model illustrates the need for control to increase the production. Figure 5 depicts the instantaneous, averaged, and equilibrium oil production for a choke opening of $Z = 60\%$. It stresses that stabilizing the flow around the equilibrium would result into a production increase.

V. CONCLUSION

A low-dimensional distributed parameters drift-flux model for two-phase slugging flow has been presented. The model equations take the form of a first-order quasilinear hyperbolic system, along with boundary conditions at both sides of the space domain. Well-posedness of this setting is proved, and the questions of one-sided boundary control and observation are discussed. A presented numerical scheme, based on the method of characteristics, allows to compute the approximate solution of the equations. The simulations stress the ability of the model to reproduce the pressure and flow rates oscillations corresponding to the slugging behavior.

Several directions for future works are considered. The problems formulated in Section III-B are an interesting challenge for the PDE control theory. They would constitute a link between a very practical industrial problem and more

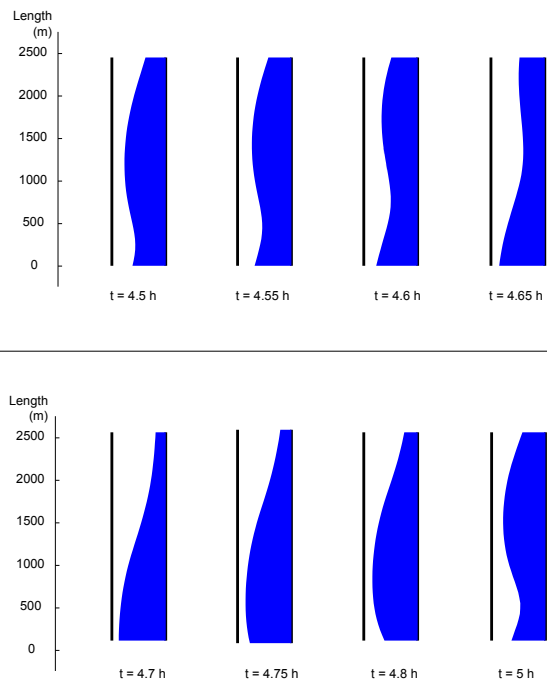


Fig. 4. Liquid mass hold-up profiles at different time instants. At $t = 4.5$ h, a “slug” is present in the middle of the pipe. It is then expelled over the next 0.2 hours, before a new slug is formed. The velocity of the flow is inhomogeneous in space and time: the slugging cycle comprises phases of acceleration and deceleration.

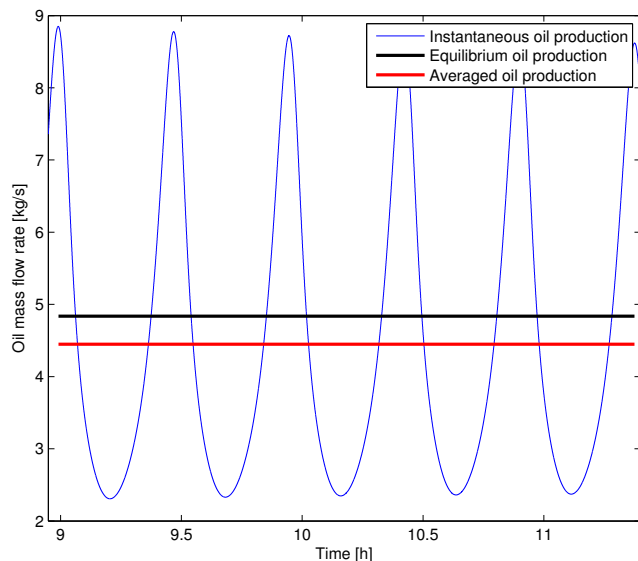


Fig. 5. Instant, average, and equilibrium oil production during slugging. The equilibrium production is higher than the average of the oscillations, but needs feedback control to be stabilized around.

theoretical topics. The recently published results by Li [26] and Krstic [25] encourage us to think that solutions may be around the corner.

Besides, concerning the numerical simulations, critical improvements must be made. The numerical scheme has difficulties when the solution approaches critical points, where the considered functions are not C^1 . In particular, the right boundary condition (15) is not Lipschitz when the topside pressure $u_2(t, L)$ reaches the separator pressure P_s . A space grid refined at the vicinity of the boundaries is considered as a possible solution to this issue. Also, more advanced comparisons with the reference multiphase flow simulator OLGATM should provide a quantitative evaluation of the performances of the model and the numerical scheme.

REFERENCES

- [1] A. M. Ansari, U. Sylvester, O. Shoham, and U. Brill. A comprehensive mechanistic model for upward two-phase flow in wellbores. *SPE Annual Technical Conference*, 1990.
- [2] G. Bastin, J.-M. Coron, and B. dAndréa Novel. Boundary feedback control and Lyapunov stability analysis for physical networks of 2x2 hyperbolic balance laws. In *47th IEEE Conference on Decision and Control*, pages 1454–1458, 2008.
- [3] H. H. J. Bloemen, S. P. C. Belfroid, Sturm W. L., and F. J. P. C. M. G. Verhelst. Soft sensing for gas lift wells. *SPE Paper*, 2006.
- [4] C. E. Brennen. *Fundamentals of multiphase flow*. Cambridge Univ Pr, 2005.
- [5] A.J. Chorin and J.E. Marsden. *A mathematical introduction to fluid mechanics*. Springer, 1993.
- [6] J.-M. Coron. *Control and Nonlinearity*. American Mathematical Society, 2007.
- [7] A. Courbot. Prevention of severe slugging in the dunbar 16' multiphase pipeline. *Offshore Technology Conference*, 1996.
- [8] F. Di Meglio, G.-O. Kaasa, and N. Petit. A first principle model for multiphase slugging flow in vertical risers. *Conference on Decision and Control*, 2009.
- [9] F. Di Meglio, G.-O. Kaasa, N. Petit, and V. Alstad. Model-based control of slugging flow: an experimental case study. *2010 American Control Conference*, 2010.
- [10] F. Di Meglio, G.-O. Kaasa, N. Petit, and V. Alstad. Reproducing slugging oscillations of a real oil well. *49th IEEE Conference on Decision and Control*, 2010.
- [11] F. P. Donohue. Classification of flowing wells with respect to velocity. *Petroleum Transactions, AIME*, 86:226–232, 1930.
- [12] E. Duret. *Dynamique et contrôle des écoulements polyphasiques*. PhD thesis, Ecole des Mines de Paris, 2005.
- [13] G. O. Eikrem, B. Foss, L. Imsland, B. Hu, and M. Golan. Stabilization of gas lifted wells. *Proceedings of the 15th IFAC World Congress*, 15, Part 1, 2002.
- [14] G. O. Eikrem, L. Imsland, and B. Foss. Stabilization of gas-lifted wells based on state estimation. *International Symposium on Advanced Control of Chemical Processes*, 2004.
- [15] J. Falcimaigne and S. Decarre. *Multiphase Production*. IFP Publications, 2008.
- [16] D. Ferre, V. Bouvier, and C. Pauchon. *TACITE Physical Model Description Manual*. Rapport IFP, 1995.
- [17] J.-M. Godhavn, M. P. Fard, and P. H. Fuchs. New slug control strategies, tuning rules and experimental results. *Journal of Process Control*, 15:547–557, 2005.
- [18] J. K. Hale. *Ordinary Differential Equations*. Wiley-Interscience, New York, 1969.
- [19] A. R. Hasan, C. S. Kabir, and M. Sayarpour. A basic approach to wellbore two-phase flow modeling. *SPE Annual Technical Conference*, 2007.
- [20] K. Havre and M. Dalsmo. Active feedback control as the solution to severe slugging. *SPE Annual Technical Conference*, 2001.
- [21] P. E. Hedne and H. Linga. Suppression of terrain slugging with automatic and manual riser choking. *Presented at the ASME Winter Annual Meeting, Dallas, Texas*, 1990.

- [22] B. Hu. *Characterizing gas-lift instabilities*. PhD thesis, Department of Petroleum Engineering and Applied Geophysics, NTNU, 2004.
- [23] L. S. Imsland. *Output Feedback and Stabilization and Control of Positive Systems*. PhD thesis, Norwegian University of Science and Technology, Department of Engineering Cybernetics, 2002.
- [24] B. Jansen, M. Daslmo, L. Nøkleberg, K. Havre, V. Kristiansen, and P. Lemetayer. Automatic control of unstable gas lifted wells. *SPE annual technical conference*, 1999.
- [25] M. Krstic and A. Smyshlyaev. Backstepping boundary control for first-order hyperbolic pdes and application to systems with actuator and sensor delays. *Systems & Control Letters*, 57(9):750 – 758, 2008.
- [26] T. T. Li. *Controllability and Observability for Quasilinear Hyperbolic Systems*, volume 3. Higher Education Press, Beijing, 2009.
- [27] N. Petit and P. Rouchon. Dynamics and solutions to some control problems for water-tank systems. *IEEE Transactions on Automatic Control*, 47(4):594–609, Apr 2002.
- [28] L. Sinègre. *Dynamic study of unstable phenomena stepping in gas-lift activated systems*. PhD thesis, Ecole des Mines de Paris, 2006.
- [29] L. Sinègre, N. Petit, and P. Menegatti. Predicting instabilities in gas-lifted wells simulation. page 8 pp., jun. 2006.
- [30] E. Storkaas. *Control solutions to avoid slug flow in pipeline-riser systems*. PhD thesis, Norwegian University of Science and Technology, 2005.
- [31] Y. Taitel, D. Bornea, and A. E. Dukler. Modelling flow pattern transitions for steady upward gas-liquid flow in vertical tubes. *AIChE Journal*, 26, No3:345–354, 1980.
- [32] T. L. Tsai, S. W. Chiang, and J. C. Yang. Characteristics method with cubic-spline interpolation for open channel flow computation. *International Journal for Numerical Methods in Fluids*, 46(6):663–683, 2004.
- [33] E. Zakarian. Analysis of two-phase flow instabilities in pipe-riser systems. *Proceedings of Pressure Vessels and Piping Conference*, 2000.

APPENDIX

The matrices corresponding to the hyperbolic form of the system read

$$A(u) = \begin{pmatrix} u_3 & 0 & 0 \\ 0 & u_3 & u_2 + \frac{(1-u_1)u_2^2}{\rho_L u_1 RT} \text{bar} \\ \frac{\rho_L RT u_1 + (1-u_1)u_2 \text{bar}}{(1-u_1)^2 u_2^2 \text{bar}^2} \rho_L RT v_\infty^2 & \frac{(\rho_L RT u_1 + (1-u_1)u_2 \text{bar})((1-u_1)u_2^2 \text{bar}^2 - \rho_L^2 u_1 RT v_\infty^2)}{\rho_L (1-u_1)u_2^3 \text{bar}^2} & u_3 - 2v_\infty \frac{\rho_L RT u_1 + (1-u_1)u_2 \text{bar}}{u_2 \text{bar}} \end{pmatrix}$$

and

$$S(z) = \begin{pmatrix} 0 \\ 0 \\ -g \sin \theta(z) \end{pmatrix}$$

The eigenvalues of A read

$$\begin{pmatrix} \lambda_1 \\ \lambda_2 \\ \lambda_3 \end{pmatrix} = \begin{pmatrix} u_3 - (1-u_1)v_\infty - \frac{\rho_L RT u_1 v_\infty}{u_2 \text{bar}} - \frac{\rho_L RT u_1 + (1-u_1)u_2 \text{bar}}{\rho_L RT (1-u_1)u_1 u_2 \text{bar}} \sqrt{u_1 (1-u_1) RT [(1-u_1)u_2^2 \text{bar}^2 - \rho_L RT u_1^2 \rho_L v_\infty^2]} \\ u_3 \\ u_3 - (1-u_1)v_\infty - \frac{\rho_L RT u_1 v_\infty}{u_2 \text{bar}} + \frac{\rho_L RT u_1 + (1-u_1)u_2 \text{bar}}{\rho_L RT (1-u_1)u_1 u_2 \text{bar}} \sqrt{u_1 (1-u_1) RT [(1-u_1)u_2^2 \text{bar}^2 - \rho_L RT u_1^2 \rho_L v_\infty^2]} \end{pmatrix}$$

and the left eigenvectors are given by

$$\begin{pmatrix} l_1(u) \\ l_2(u) \\ l_3(u) \end{pmatrix} = \begin{pmatrix} 1 & \frac{(1-u_1)^2 u_2 \text{bar}^2}{\rho_L RT \rho_L v_\infty^2} - \frac{(1-u_1)u_1}{u_2} & -\frac{(1-u_1)u_2 \text{bar} \sqrt{u_1 (1-u_1) RT [(1-u_1)u_2^2 \text{bar}^2 - \rho_L RT u_1^2 \rho_L v_\infty^2]}}{\rho_L^2 R^2 T^2 v_\infty^2 u_1} - \frac{(1-u_1)^2 u_2 \text{bar}}{\rho_L RT v_\infty} \\ 1 & 0 & 0 \\ 1 & \frac{(1-u_1)^2 u_2 \text{bar}^2}{\rho_L RT \rho_L v_\infty^2} - \frac{(1-u_1)u_1}{u_2} & \frac{(1-u_1)u_2 \text{bar} \sqrt{u_1 (1-u_1) RT [(1-u_1)u_2^2 \text{bar}^2 - \rho_L RT u_1^2 \rho_L v_\infty^2]}}{\rho_L^2 R^2 T^2 v_\infty^2 u_1} - \frac{(1-u_1)^2 u_2 \text{bar}}{\rho_L RT v_\infty} \end{pmatrix}$$